the basis of variations in the heat flow values has been demonstrated in the southwestern part of the

region where anomalies trace the extension of the faults through the slope of the Ukrainian Shield.

Modeling of the nonlinear resonant response in sedimentary rocks

© *V. Vakhnenko[1], O. Vakhnenko[2], J. TenCate[3], T. Shankland[3], 2010*

[1]Institute of Geophysics, National Academy of Sciences of Ukraine, Kiev, Ukraine
vakhnenko@ukr.net
[2]Institute for Theoretical Physics, National Academy of Sciences of Ukraine, Kiev, Ukraine
vakhnenko@bitp.kiev.ua
[3]Los Alamos National Laboratory, New Mexico, USA
tencate@lanl.gov
shankland@lanl.gov

Sedimentary rocks, particularly sandstones, are distinguished by their grain structure in which each grain is much harder than the intergrain cementation material [Guyer, Johnson, 1999]. The peculiarities of grain and pore structures give rise to a variety of remarkable nonlinear mechanical properties demonstrated by rocks, both at quasistatic and alternating dynamic loading [Guyer, Johnson, 1999; TenCate, Shankland, 1996; TenCate et al., 2000; Darling et al., 2004]. We suggest a model for describing a wide class of nonlinear and hysteretic effects in sedimentary rocks at longitudinal bar resonance. In particular, we explain: hysteretic behaviour of a resonance curve on both its upward and downward slopes; linear softening of resonant frequency with increase of driving level; gradual (almost logarithmic) recovery of resonant frequency after large dynamical strains; and temporal relaxation of response amplitude at fixed frequency. Starting with a suggested model, we predict the dynamical realization of end-point memory in resonating bar experiments with a cyclic frequency protocol. These theoretical findings were confirmed experimentally at Los Alamos National Laboratory.

A reliable probing method widely applied in resonant bar experiments is to drive a horizontally suspended cylindrical sample with a piezoelectric force transducer cemented between one end of the sample and a massive backload, and to simultaneously measure the sample response with a low-mass accelerometer attached to the opposite end of the bar[2,4]. The evolution equation for the field of bar longitudinal displacements u as applied to above experimental configuration we write as follows

$$\rho \frac{\partial^2 u}{\partial t^2} = \frac{\partial \sigma}{\partial x} + \frac{\partial}{\partial x}\left[\frac{\partial \mathfrak{I}}{\partial(\partial^2 u / \partial x \partial t)} \right]. \quad (1)$$

Here we use the Stokes internal friction associated with the dissipative function $\mathfrak{I} = (\gamma/2)\times$ $\times[\partial^2 u / \partial x \partial t]^2$. The quantities ρ and γ are, respectively, mean density of sandstone and coefficient of internal friction. The stress-strain relation ($\sigma - \partial u/\partial x$) we adopt in the form

$$\sigma = \frac{E \operatorname{sech}\eta}{(r-a)\left[\cosh\eta\, \partial u / \partial x + 1\right]^{a+1}} -$$

$$- \frac{E \operatorname{sech}\eta}{(r-a)\left[\cosh\eta\, \partial u / \partial x + 1\right]^{r+1}}, \quad (2)$$

which for $r > a > 0$ allows us to suppress the bar compressibility at strain $\partial u/\partial x$ tending toward $+0 - \operatorname{sech}\eta$. Thus, the parameter $\operatorname{coch}\eta$ is assigned for a typical distance between the centers of neighboring grains divided by the typical thickness of intergrain cementation contact.

The indirect effect of strain on Young's modulus E, as mediated by the concentration c of ruptured intergrain cohesive bonds, is incorporated in our theory as the main source of all non-trivial phenomena. We introduce a phenomenological relationship between defect concentration and Young's modulus. Intuition suggests that E must be some monotonically decreasing function of c, which can be expanded in a power series with respect to a small deviation of c from its unstrained equilibrium

value c_0. To lowest informative approximation we have

$$E = (1 - c/c_{cr})E_+ . \tag{3}$$

Here c_{cr} and E_+ are the critical concentration of defects and the maximum possible value of Young's modulus, respectively. The equilibrium concentration of defects $c\sigma$ associated with a stress σ is given by

$$c_\sigma = c_0 \exp(\upsilon\sigma/kT) , \tag{4}$$

where the parameter $\upsilon > 0$ characterizes the intensity of dilatation. Although formula (4) should supposedly be applicable to the ensemble of microscopic defects in crystals, it was derived in the framework of continuum thermodynamic theory that does not actually need any specification of either the typical size of an elementary defect or the particular structure of the crystalline matrix. For this reason we believe it should also work for an ensemble of mesoscopic defects in consolidated materials, provided that for a single defect we understand some elementary rupture of intergrain cohesion.

Fig. 1 shows typical resonance curves, i. e., dependences of response amplitudes R (calculated at $x=L$) on drive frequency $f=\omega/2\pi$, at successively higher drive amplitudes D. Solid lines correspond to conditioned resonance curves calculated after two frequency sweeps were performed at each driving level in order to achieve repeatable hysteretic curves. The dashed line illustrates an unconditioned curve obtained without any preliminary conditioning. Arrows on the three highest curves indicate sweep directions. This results of the computer simulations were adapted to experimental conditions appropriate to the data obtained by TenCate and Shankland for Berea sandstone [TenCate, Shankland, 1996].
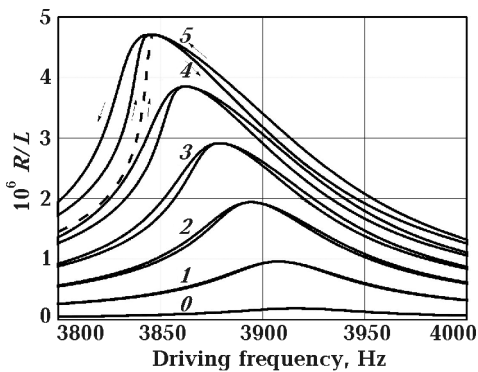

Fig. 1. Resonance curves $j = 0, 1, 2, 3, 4, 5$ at successively higher driving amplitudes $D_j = 3.8(j + 0.2\delta_{j0})10^{-8} L$.
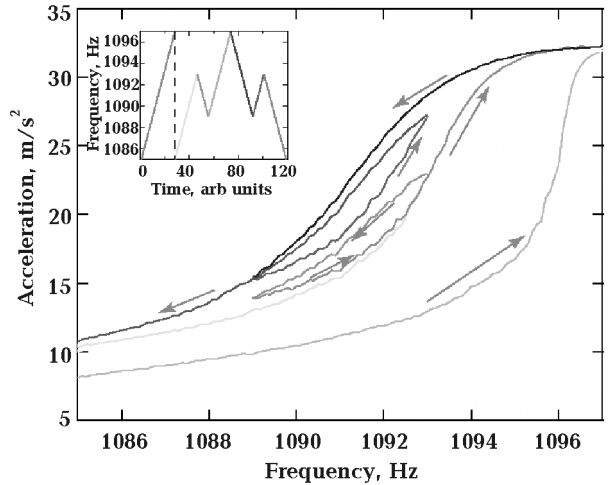

Fig. 2. Recovery of resonant frequency f_r to its maximum limiting value f_0.

Fig. 2 shows the gradual recovery of resonant frequency f_r to its maximum limiting value f_0 after the bar has been subjected to high amplitude conditioning and conditioning was stopped. We clearly see the very wide time interval $10 \le (t - t_c)/t_0 \le 1000$ of logarithmic recovery of the resonant frequency (Fig. 2), in complete agreement with experimental results. Here t_c is the moment when conditioning switches off and $t_0=1s$ is the time scaling constant. Curves $j=1, 2, 3$ on lower Fig. 2 correspond to successively high water saturations $s_j=0.05(2_j-1)$.

The question of whether an effect similar to the end-point (discrete) memory that is observed in quasi-static experiments with a multiply-reversed loading-unloading protocol (see [Darling et al., 2004] and references there) could also be seen in resonating bar experiments with a multiply-reversed frequency protocol has been raised in [Vakhnenko et al., 2006] and was first examined theoretically. The graphical results of this investigation are presented in Fig. 16 in [Vakhnenko et al., 2005] One of the features of dynamical end-point memory, defined here as the memory of the previous maximum amplitude of alternating stress, is seen as small loops inside the major loop. The starting and final points of each small loop coincide, which is typical of end-point memory.

Following the theoretical results, we performed experimental measurements to verify our prediction [Vakhnenko et al., 2005]. The sample bar was a Fontainebleau sandstone and the drive level produced a calculated strain of about at the peak. Fig. 3 shows the low frequency sides of resonance curves
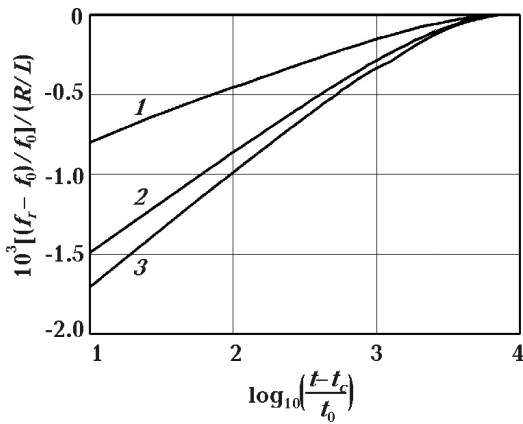
Fig. 3. The low frequency sides of experimental reso-
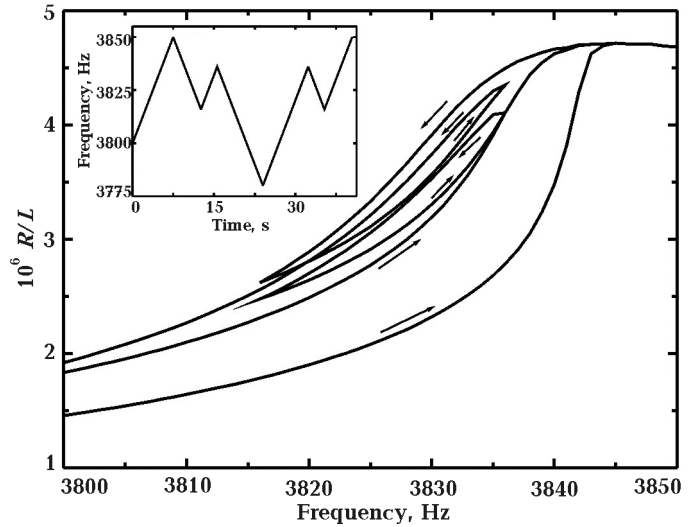nance curves for Fontainebleau sandstone.

Fig. 4. The low frequency sides of the resonance curves calcu-
lated for Berea sandstone.

that correspond to the frequency protocol given on inset of Fig. 3. We clearly see that the beginning and end of each inner loop coincide, i. e., a major feature of end-point memory.

The experimental results for the Fontainebleau sandstone shown in Fig. 3 were reproduced by using our model equations though with constants (including a state equation) developed for Berea sandstone [Vakhnenko et al., 2005]. We note the good qualitative agreement between the experimental (Fig. 3) and the theoretical (Fig. 4) curves sugges-

ting that our physical model is appropriate for both sand-stones.

Hence, the suggested model enables us to describe correctly a wide class of experimental facts concerning the unusual dynamical behaviour of such mesoscopically inhomogeneous media as sand-stones. Moreover, as it is shown below, we have predicted the phenomenon of hysteresis with end-point memory in its essentially dynamical hyposta-sis. These theoretical findings were con-firmed experimentally at Los Alamos National Laboratory.

References

Darling T. W., TenCate J. A., Brown D. W., Clausen B., Vogel S. C. Neutron diffraction study of the contribution of grain contacts to nonlinear stress-strain behavior // Geophys. Res. Lett. — 2004. — **31**. — P. L16604(4).

Guyer R. A., Johnson P. A. Nonlinear mesoscopic elasticity: Evidence for a new class of materials // Physics Today. — 1999. — **52**. — P. 30—35.

TenCate J. A., Shankland T. J. Slow dynamics in the nonlinear elastic response of Berea sandstone // Geophys. Res. Lett. — 1996. — **23**. — P. 3019—3022.

TenCate J. A., Smith E., Guyer R. A. Universal slow

dynamics in granular solids // Phys. Rev. Lett. — 2000. — **85**. — P. 1020—1024.

Vakhnenko O. O., Vakhnenko V. O., Shankland T. J. Soft-ratchet modelling of end-point memory in the nonlinear resonant response of sedimentary rocks // Phys. Rev. B. — 2005. — **71**. — P. 174103(14).

Vakhnenko V. O., Vakhnenko O. O., TenCate J. A., Shankland T. J. Dynamical realization of end-point memory in consolidated materials // Innovations in nonlinear acoustics: ISNA17—17th International Symposium on Nonlinear Acoustics. — AIP Conference Proceedings. — 2006. — **838**. — P. 124—127.